Computer design of perfect additives for perylene red

Peter Erk
Josef Hetzenegger
Arno Böhm

In the process of designing high-performance additives for perylene red molecular modeling techniques were used to determine the crystal habit of C. I. Pigment Red 179. With respect to the structure of the dominating crystal faces perylene-3,4-dicarboxylic acid imides (PDCIs) were chosen as potential tailormade additives. Advanced modeling studies as well as adsorption and crystallization experiments provided excellent proof of this hypothesis.

PDCI based additives are now used as powerful dispersants for BASF's perylene red brands. As genuine pigment additives they work in both, waterborne and high solid-systems, greatly improving rheological and coloristic properties.

Introduction

The rheological properties of paints, the stability of pigment dispersions and the optical properties of the resulting coatings are closely related to colloidal stabilization of pigmentary primary particles [1]. Various models exist to rationalize stabilization mechanisms for pigment dispersions and hence to guide the creation of efficient paint formulations.

Most of these models rely on the stabilizing effect of an amphiphilic dispersing agent. The head group of the dispersant binds to the pigment surface while the tail provides the desired steric or electrostatic stabilization or a better compatibility with the surrounding medium. Up to date many successful applications of this concept have been realized using molecular, oligomeric or polymeric dispersing agents [2].

The anchoring head groups of these dispersants are usually designed to complement the polar nature of the pigment particle surface enabling pigment-dispersant interaction via coulomb forces, salt formation or hydrogen bonds. In the case of non-polar pigment surfaces the use of synergists (as exemplified in [3]) may be the most promising approach. In this

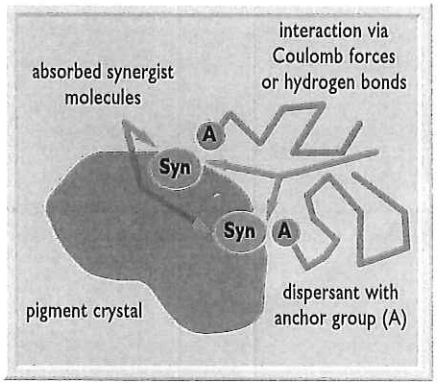

Fig. 1: Schematic representation of a synergist/dispersant-modified pigment

concept chemically derivatised pigment moieties act as perfectly matching anchor groups *(Fig. 1)*. They enable the attachment of a conventional dispersant through specific interactions with suitable substituents.

Analysis of *Fig. 1* in search for general guidelines on how to make a paint system work, however, reveals that no molecularly defined structure/effect relationships exist except for the design of the synergist.

Synergists can be designed according to the principles depicted for tailormade additives which are used as habit modifiers in crystallizations [4]. This concept provides a highly efficient strategy to outline compounds suitable for specific interactions with crystal faces. Accordingly, one can construct tailormade additives by fitting them to the structure of the crystal face to interact with.

Thus a straightforward approach to designing tailormade additives is the use of a modified substrate molecule carrying an additional substituent to repel other molecules from the surface (growth inhibitor on face A in *Fig. 2*). Alternatively, growth inhibition can be achieved by a compound whose molecular geometry and interaction sites on one side match up with the surface structure whereas the opposite side of the additive molecule mismatches with the crystallizing substrate (see face B in *Fig. 2*).

To employ this clear cut concept in the sense of a rational design strategy information about the chemical structure of the pigment surface is inevitably needed, but hard to elucidate from nanosized crystals.

To collect structural surface informations we used computational chemistry methods that offer a powerful means to derive the morphology of organic molecular crystals from the crystal structure and to examine the molecular landscapes of the crystal faces using computer graphic visualization techniques.

Hence, computational methods play an important role in the design strategy presented here. They involve crystal structure determination of the pigment (if necessary), checking of force field applicability, calculation of crystal habit, analysis of surface structures and determination of additive efficacy. Finally, they enabled us to locate new key structures for technical applications.

As a first example for this strategy we describe the development of a new versatile synergistic additive applicable to N,N'-dimethyl-perylene-3,4-9,10-tetracarboxylic acid di-imide (DMePTCDI, C. I. Pigment Red 179), the classical perylene red.

Experimental

All calculations have been performed with the modelling package "Cerius²" [5]. Unless otherwise noted we used the default setup of version 1.6. In all force field-based methods the "Dreiding 2.21" [6] parameter set has been applied. Charges were taken from MNDO-ESP calculations and scaled by a factor of 1.422 [7].

The synthetic procedures to obtain the materials used in this work are described in US patent 5,472,494.

Crystallization experiments were carried out in glass vessels with analytical grade solvents or solutions of additives using ball-milled Pigment Red 179 as feed. Carefully purified P. R.179 and multiply recrystallized MePDCI were used. All experiments were repeated twice.

Fig. 2: General construction scheme for face-selective additives

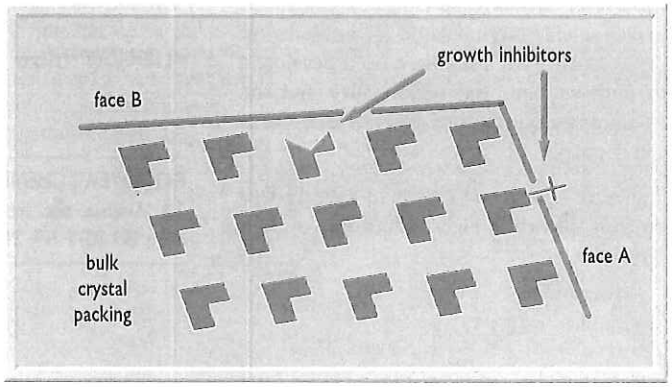

Results and discussion

Packing energy calculations

Crucial for the correct determination of crystal habits by force field methods is an initial check of the force field in use. To investigate the ability of the "Dreiding 2.21" force field for describing perylene red we optimized the crystal structure of P.R.179 starting from experimental data [8]. P.R.179 crystallizes in the common space group $P2_1/c$, the planar molecule occupying the centre of in-

LIFELINE

Dr. *Peter Erk* studied chemistry at Würzburg University/Germany where he also received his PhD. Afterwards, he worked on metalloporphyrins at Stanford University, USA. Since 1991 he is with BASF in Germany where he is working on R & D in the colorants laboratory. The technology of crystals is the focus of his research.

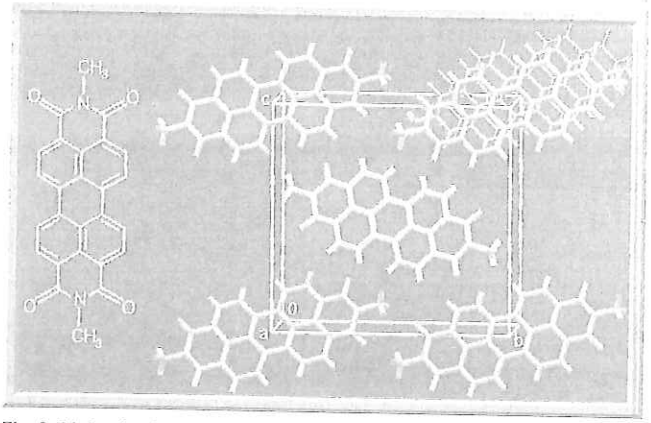

Fig. 3: Molecular formula and crystal packing of P. R.179

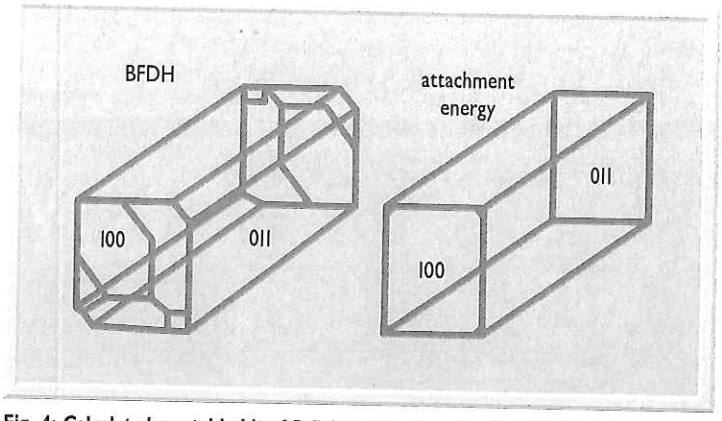

Fig. 4: Calculated crystal habit of P. R.179; left: according to BFDH; right: attachment energy calculation result; unit cell is given for comparison

version and stacking uniformly along the a-axis. So far no polymorphs of P.R.179 are described in the literature.

To eliminate inaccuracies originating from hydrogen atom positioning in the experimental structure we used the molecular geometry derived from force field calculations. Placing the molecule into the experimental unit cell and refining both, molecular and cell geometry, by minimizing the force field energy did not induce major changes in the packing arrangement. The root mean square deviation of experimental and calculated cell geometry amounts to 85 pm (2.5 %). According to our experience on molecular crystals this minor deviation fits well within the expected error marks of force field methods.

Crystal habit determination

For more than a century scientists have worked on simulation methods to derive crystal morphologies on the base of internal crystal structures. Within the last decade substantial progress in this field [9,10] was manifested in the development of readily available computer codes for attachment energy calculation [11] and automated periodic bond chain (PBC) analysis [12].

We use two methods which are both incorporated into "Cerius²". The simplest method to derive crystal morphologies follows the *Bravais-Friedel-Donnay-Harker* (BFDH) model which only takes the lattice geometry and symmetry into account [13]. In this model, the morphological importance of a face (hkl) is simply equal to the symmetry extinction corrected interplanar spacing of that face.

The second method has been worked out by *Hartmann* and *Bennema*, who demonstrated that for crystals growing at low supersaturation, the relative growth rate of a face (hkl) is proportional to the attachment energy E_{att} which is released as a crystal slice attaches to the face from infinite distance [14]. The program "Habit" [11] allows to calculate attachment energies of all possible crystal faces for a given structure.

Usually BFDH is used to give a coarse grain impression of the crystal form to be expected, while attachment energy calculations provide more accurate results by taking the strength and directionality of intermolecular interactions into account.

According to both BFDH and attachment energy calculations, the equilibrium crystal habit of P.R.179 is represented by a prismatic rod with an aspect ratio of ≈ 3 *(Fig. 3)*. These results are in excellent agreement with experimental observations. The overall shape of crystals grown from solvents like xylene or phenol appears as according to the modelling results.

As expected for a stacked planar aromatic molecule, the main growth direction coincides with the stacking direction along the a-axis. According to the attachment energies listed in *Table 1*, the system gains more than twice the energy by growing in the (100) direction as compared to (011). Subsequently, the (011) face accounts for more than 80 % of the crystal surface.

Due to the thermodynamic assumptions of the model, calculated habiti mirror the crystal shape to be expected under undisturbed equilibrium conditions. The presence of strongly interacting solvents or impurities can dramatically change the observed habit and bring up faces which do not occur otherwise. E. g. crystallization from sulfuric acid yields coffin-like crystals with a more pronounced (020) face, whereas common impurities stabilize the (102) face.

Additive design

The unequivocal results of the morphology calculations provide the information required to build up, visualize and analyse the surface structure of P.R.179. They emphasize that effective additives should match with the dominating (011) face.

A projection of (100) through the crystal terminated by the (011) and symmetry related faces clarifies the surface structure of the (011) face *(Fig. 5)*. The P.R.179 molecules occupy two different crystallographic positions (A and B) in the (011) face.

The analysis of the surface structure for atom positions to be substituted (usually those sticking out of the surface) indicates to use either a PTCDI derivative functionalized at certain positions on the perylene ring (2-X-PTCDI) or an asymmetrically N,N'-disubstituted PTCDI derivative (R,R'-PTCDI), *Fig. 6*.

A more promising approach takes advantage of molecules derived from truncating the P.R.179 structure. Additives of this kind fit well into both positions of the (011) face. Possible structures according to this concept are N-Methyl-perylene-3,4-dicarboxylic acid imide (MePDCI) or N-Methyl-naphthalene-1,8-dicarboxylic acid imide (MeNDCI).

In the case of MePDCI even 9-substituted derivatives may be embedded into both positions of the (011) face whereas a 4-substituted NDCI derivative cannot be placed in the surface due to steric hindrance caused by the substituent.

To roughly estimate the activity of these additive structures, we calculated the intermolecular enthalpy gained by embedding PDCI and NDCI type structures into the (011) face and compared these to the corresponding values for P.R.179 itself *(Table 2)*. To exclude artificial strain all embedded molecules were fully relaxed in a force field minimization. This relaxation led to a slight displacement of the molecules. In position A all compounds listed in *Fig. 8* moved by 70±5 pm away from the surface. The overall displacement for position B calculates to 46±2 pm except the 9-sulfonated HPDCI whose bulky sulfonate group causes a shift of 69 pm *(Fig. 7)*.

The energy calculations show that PDCI derivatives – regardless of N-methyl substitution and the existence of a sulfo group in 9-position – bind to the surface with approximately 90 % of the interaction energy a P.R.179 molecule itself would deliver. How-

Table 1: Listing of relative surface areas and surface energetics for BFDH and attachment energy (*Eatt*) calculation (AEC)

Face (hkl)	BFDH area [%]	AEC area [%]	E_{att} [kcal/growth unit]
0 1 1	76.0	83.5	37.3
1 0 0	7.31	16.2	94.5
0 2 0	6.98	0.0	62.5
1 1 1	6.70	0.0	107.4
1 1 0	2.5	0.13	104.0
1 0 2	0.0	0.09	98.5
1 0 2	0.50	0.05	112

Table 2: Intermolecular entalpies (van-der-Waals + Coulomb, ΔH_{emb}) and displacement of compounds embedded into the (011) face of P.R. 179. Values have been derived from force field relaxation of the compounds in an array of 7 x 6 x 3 molecules cut from the bulk crystal structure. For assignment to positions A and B see *fig. 5*.

Compound	ΔH_{emb} A [kcal/mol]	ΔH_{emb} B [kcal/mol]	displacement [Å]
P.R. 179 (unrelaxed)	66.6	66.5	0
P.R. 179	94.5	88.7	0.46 B
MePDCI	82.9	80.4	0.47 B
HPDCI	76.4	81.3	0.46 B
HPDCI-9-SO_3-H	83.6	85.8	0.69 B
MeNDCI	57.6	54.7	0.71 A
HNDCI	52.3	56.3	0.70 A

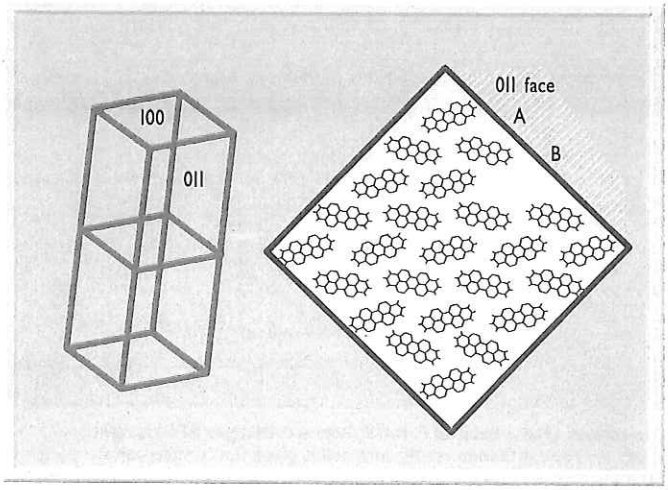

Fig. 5: Cross section of a P. R.179 crystal projected parallel to (100); A and B denote different molecule orientations in the (011) face

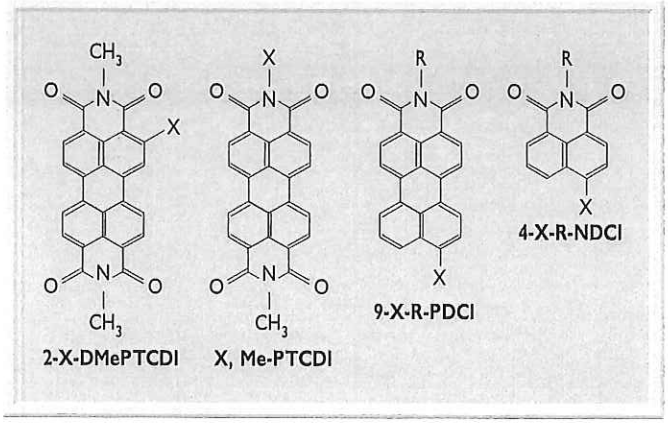

Fig. 6: Scheme with possible additive structures

ever, the embedding enthalpy of NDCIs amounts to only 60 % of this benchmark value.

Though these calculations do not yield anything close to an adsorption enthalpy, they reflect fairly well the relative ability of a molecule to bind to a surface site. Consequently, the embedding enthalpies of *Table 2* can be considered as a useful measure to rank possible synergist candidates.

With respect to the technical requirements for modern pigment brands based on P.R.179 (high chromaticity, yellowish hue) we choose the PDCI system as the most promising approach for further investigations.

Crystal growth inhibition

To prove the modelling based hypothesis described in the previous chapter we investigated the influence of MePDCI on the crystallization behavior of P.R.179 in various solvents.

Crystallization of ball-milled P.R.179 in phenol at 100 °C yields prismatic rods of several microns length *(Fig. 8)*. The crystals show clear cut faces without any significant difference compared to the equilibrium habit.

Addition of MePDCI to the otherwise identical crystallization process changes the morphology dramatically. The most striking effect is the reduction in crystal size which correlates fairly well with the amount of MePDCI in solution. The addition of 8 % MePDCI to the experiment described above causes the overall particle size to drop well below the 1 µm limit *(Fig. 9)*.

The changes in particle size are accompanied by delicate modifications of the crystal habit. Crystals grown or ripened in the presence of MePDCI look like grains of rice with an elongated oval shape *(Fig. 9)*. Assuming that the elongated axis in these grain-like crystals corresponds to the genuine needle axis of P.R.179, the rounded ends should be terminated by a series of medium energy faces or facets (hkl), presumably of the type h, k, l > 0. The emergence of these faces may be attributed to the stabilizing effect of the PDCI additive.

To cross-check our modelling ranking *(Fig. 8)* MeNDCI has been added to the rather brute-force ripening procedure in phenol. In this case no defined morphology changes were observed. The use of MeNDCI in crystallizations performed in xylene induces similar but very moderate changes in the crystal morphology of P.R.179 compared to MePDCI. In general, one finds the same sequence (MePDCI ≥ HPDCI >> MeNDCI > HNDCI) in growth inhibiting performance as predicted by the modelling results *(Fig. 8)*.

Adsorption measurements

Consistently with the modeling results, the described crystallization experiments give proof of the surface specific activity of PDCI type additives, thus referring to the thermodynamics of additive attachment to surface sites. As can be seen from *Fig. 8* the interaction enthalpy of 9-sulfonated HPDCI is in the order of MePDCI and other highly surface active PDCI derivatives. Considering the requirements for a synergistic additive given in the introduction HPDCI-9-SO_3H qualifies as a potent synergist candidate.

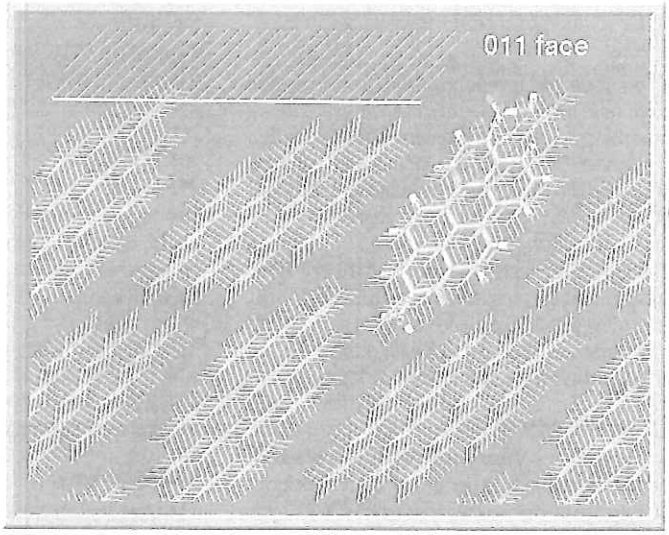

Fig. 7: Minimum energy position of HPDCI-9-SO_3H embedded into the (011) face

Many synergists derived from substituted pigment molecules have low solubilities in the commonly used application media. These drawbacks in their applicability usually have to be overcome by adding the synergist prior to milling operations in the formulation process chain. All PDCI based synergists examined in this work show moderate solubility in organic solvents and/or water. On purpose to monitor the activity of PDCI additives in solution and to follow the uptake of the synergist by a pigment dispersion we performed some simple adsorption experiments.

To follow the adsorption of HPDCI-9-SO_3H (0.5 % solution in deionized water) onto P.R.179 (400 nm particles, additive/pigment ratio 1/20) at ambient temperature under no shear conditions the concentra-

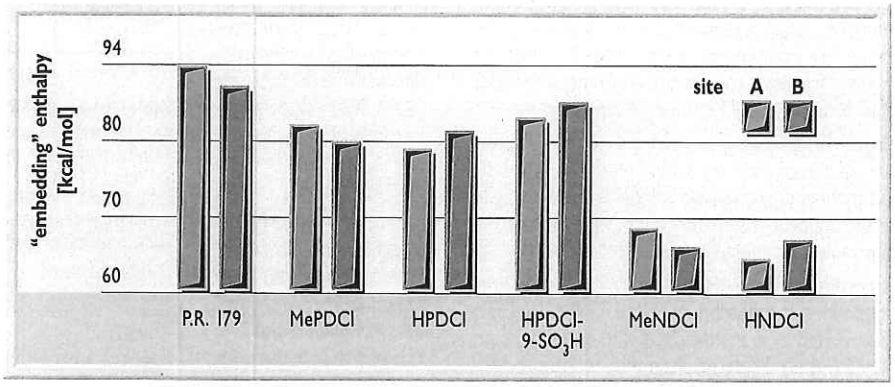

Fig. 8: Intermolecular enthalpies (van-der-Waals + Coulomb, ΔH_{emb}) of compounds embedded into the (011) face of P. R.179. Values have been derived from force field relaxation of the compounds in an array of 7x6x3 molecules cut from the bulk crystal structure (Fig. 6). For assignment to positions A and B see Figure 5

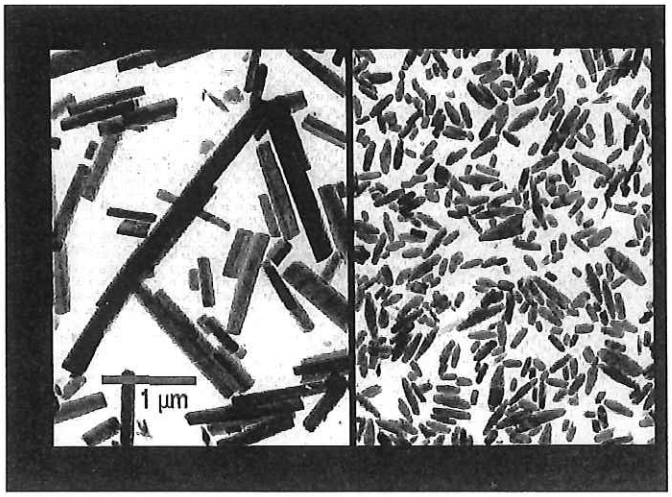

Fig. 9: Transmission electron micrographs of P. R.179 crystallized from phenol in the presence of no (left) and 8 % MePDCI (right)

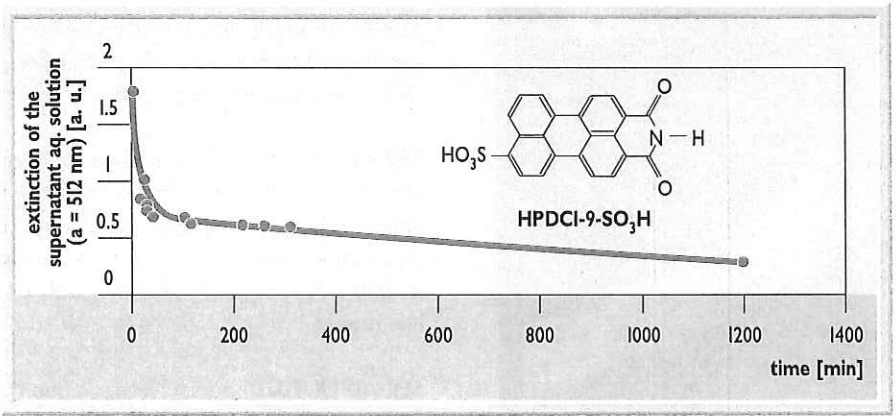

Fig. 10: Uptake of HPDCI-9-SO_3H by pigment dispersions from aqueous solution under no shear conditions followed by UV/Vis-spectroscopy

tion of the additive in the supernatant solution was measured UV/Vis-spectroscopically over time. Samples of the pigment suspension serum were taken within constant time intervals. After removal of residual pigment particles by membrane filtration all samples were centrifuged prior to measurement.

Usually, the uptake of HPDCI-9-SO_3H by the pigment is preceded by an initial offset period whose duration and characteristics strongly depend on the primary particle size and the agglomeration level of the pigment. The presence of hydrophobic coadditives, e. g. grinding aids, also induces an offset period which may be explained as a deagglomeration step prior to adsorption.

The example depicted in *Fig. 10* exhibits almost no offset period. This observation matches up with our expectations for the chosen particle size range showing no or a negligible agglomeration grade only. The concentration of HPDCI-9-SO_3H in solution decreases rapidly after addition of the pigment reaching asymptotically a final value of roughly 1/10 of the initial extinction in the current experiment *(Fig. 10)*.

No desorption of HPDCI-9-SO_3H from the pigment surface could be observed in solvents where P.R.179 shows no or little recrystallization tendency, thus underlining the quasi-irreversible character of the HPDCI-9-SO_3H adsorption. The time-dependency of the additive uptake ideally reflects the slope of a Langmuir-type adsorption isotherm. These experiments demonstrate impressively the strong affinity of HPDCI-9-SO_3H to P.R.179 crystal surfaces.

Properties of pigment formulations

In order to prove the technical applicability of our rational approach towards tailormade pigment additives we finally investigated pigment preparations in various paint formulations with special emphasis on modern waterborne and high solid-coating systems. E. g. pigment formulations with HPDCI-9-SO_3H show a greatly improved flocculation stability in waterborne coatings which might be due to an ionic stabilization of the pigment dispersion. To prepare these formulations the additive may be added at any point in the processing of the pigment.

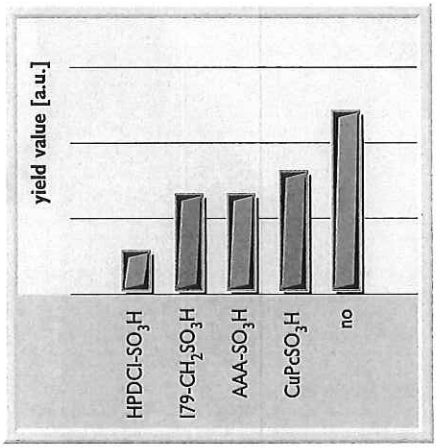

Fig. 11: Comparative viscosity yield values of formulations (based on a P. R.179 pigment with an average particle size of 50 nm) using different synergists (+ basic dispersant) in a typical high solid-system

In solvent borne coating systems with medium or high solids content HPDCI-9-SO_3H acts not only as a dispersion stabilizing agent but also takes part as a dispersing aid in the paint preparation process. In this case the timing of the synergist addition during the pigment processing occurs as a crucial step with respect to the performance of the pigment formulation.

The adsorption of HPDCI-9-SO_3H to P.R.179 results in an acid group covered pigment surface which is designated to bind basic anchor groups of common dispersants, e.g. those required to improve the rheological properties of coating systems with high solids content. In contrast to other additives that may or may not be able to interact specifically with P.R.179 surfaces, HPDCI-9-SO_3H adsorption provides a modification of the pigments surface which allows basic dispersants to work extremely well and fully develop their steric stabilization power *(Fig. 11)*. E. g. yield values accessible with HPDCI-9-SO_3H modified pigments reach close to zero.

In general HPDCI-9-SO_3H modified P.R.179 pigments show greatly improved coloristic properties in all coating systems. The improved performance of these pigments is expressed by a higher color strength, a more yellowish color shade, a better color saturation and hence distinctively enlarging the technical scope of perylene red.

Conclusions

PDCI based synergists represent state-of-the-art additives for C.I. Pigment Red 179. Their development has been guided by computational studies. These worked successful in the prediction of the crystal habit, the analysis of the surface structure and the calculation of additive efficacy.

In combination with carefully selected experiments computational methods offer an advanced knowledge base for the rational design of surface specific tailormade additives. Subsequently, they are regarded as an efficient means for adapting the surface properties of pigments to the demands of future applications.

We like to thank *P. Blaschka, Dr. T. Clemens, Dr. C. Carpenter* and *Dr. J. Schröder* for helpful discussions, *W. Best* for colorimetry measurements and *Dr. W. Fabian* for a gift of highly purified Pigment Red 179. The technical assistance of *W. Helfer, T. Saffert, M. Schröder, G. Becker, D. Zach* and *S. Burg* is gratefully acknowledged.

REFERENCES

[1] *R. Iden*, Spektrum d. Wiss. 8 (1994), p. 96
[2] *B. G. Hays*, Am. Ink Maker, Nov. (1990), p. 28
[3] *J. D. Schofield*, J. Oil Col. Chem. Assoc. 74 (1991), p. 204
[4] *I. Weissbuch, R. Popovitz-Biro, M. Lahav, L. Leiserowitz*, Acta Crystallogr. B 51 (1995), p. 115.
[5] "Cerius²", Version 1.6, Molecular Simulations Inc., 1994.
[6] *S. L. Mayo, B. D. Olafson, W. A. Goddard III*, J. Phys. Chem. 94 (1990), p. 8897.
[7] *J. J. P. Stewart*, MOPAC 6.0, QCPE # 455.
[8] *E. Hädicke, F. Graser*, Acta Crystallogr. C 42 (1986), p. 189.
[9] *Z. Berkovitch-Yellin*, J. Am. Chem. Soc. 107 (1985), p. 8239.
[10] *K. J. Roberts, E. M. Walker*, Solid State & Material Science 1 (1996), p. 506.
[11] *G. Clydesdale, R. Docherty, K. J. Roberts*, Comp. Phys. Commun. 64 (1991), p. 311.
[12] *C. S. Strom, R. F. P. Grimbergen, I. D. K. Hiralal, B. G. Koenders, P. Bennema, J.* Cryst. Growth 149 (1995), p. 96.
[13] *J. D. H. Donnay, D. Harker*, Am. Mineral. 22 (1937), p. 446.
[14] *P. Hartmann, P. Bennema*, J. Cryst. Growth 49 (1980), p. 145.